Thermal Conductivity of Butane at High Pressure: Correlation with Other Gases

F. R. KRAMER[1] and E. W. COMINGS[2]
Purdue University, Lafayette, Ind.

THERMAL conductivities of dense gases are important in engineering design and in the theoretical interpretation of molecular interaction. Much of the available data is for simple, compact molecular structures, while measurements for more complex structures are scanty.

The dense gas theory for spherical molecules by Chapman and Enskog (2) offers only limited success in predicting the effect of pressure on thermal conductivities of simple gases (16, 17). However, Comings and Nathan (4), utilizing P-V-T and high pressure viscosity data in conjunction with the dense gas theory, constructed a generalized chart of thermal conductivity ratio *vs.* reduced temperature and pressure. Lenoir and Junk (7, 12, 13) measured the thermal conductivities of a number of simple gases up to a reduced pressure of about six, and Lenoir, Junk, and Comings (14) adjusted the previous correlation to conform with these measured values. It was found later that ethane deviated by as much as 40% from the adjusted (7) correlation. Measurements by Leng (10, 11) on propane above the critical temperature showed further deviations of 60%. His measurements were conducted in both gas and liquid phases in the vicinity of the critical point and a previously unobserved behavior was noted in the liquid phase in this region. An attempt was made to extend the Comings and Nathan correlation for spherical molecules by adding a correction chart which introduced a third parameter, the total number of degrees of vibrational freedom in the more complex molecules. Inadequate data for complex molecules prevented the testing and perfection of this correlation.

In this investigation a thermal conductivity cell, capable of measurements at higher temperatures and pressures, was developed. The thermal conductivity of butane was measured in the liquid and gas phases in the region of the critical point, and in the single phase region at pressures well above the critical. An improved generalized correlation is presented for complex gases.

APPARATUS

The Thermal Conductivity Cell. The concentric cylinders cell design is shown in Figure 1. It was based on an original design by Lee (9), and was a modification of that reported by Comings, Lee, and Kramer, (3). The cell was calibrated at 1 atm. with gases of known thermal conductivity. It consisted of three concentric cylinders, the outer two of copper and the inner of Supramica—a synthetic glass-bonded mica material. A platinum wire of small diameter was wound into a milled spiral groove in the inner cylinder and served both as a resistance thermometer and heating element. This cylinder fitted tightly into the intermediate copper cylinder, which fitted into a hole in the outer copper cylinder with a radial clearance of 0.006 inch. The cell was contained in the cavity of a high pressure vessel. The outer cylinder made direct, metallic contact with the walls of the vessel by means of brass spring clips and copper foil packing. Heat generated in the platinum coil flowed radially outward through the copper cylinders and the 0.006-inch gas gap and then on through the bomb walls to the constant temperature oil bath in which the bomb was immersed. Axial heat flow was minimized by Supramica end insulation. The heating

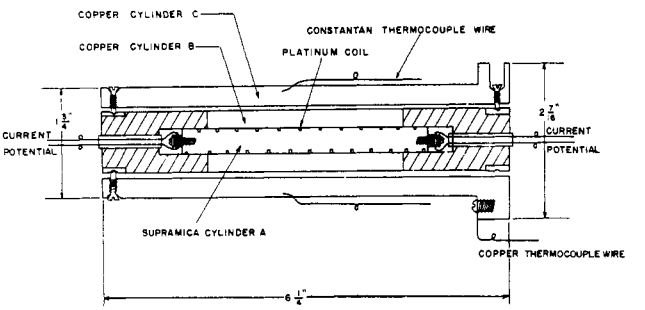

Figure 1. Thermal conductivity cell

current was supplied by four 6-volt storage batteries wired in parallel. By measuring the voltage drop across the platinum coil and the current passing through it, the heat generated and the temperature of the coil were determined. A thermocouple in the outer cylinder permitted the temperature drop from coil to outer cylinder to be determined. The temperature differences across the gas layer were about 2° F. The quotient $\Delta t/Q$ where Δt is the temperature difference from the platium coil to the thermocouple and Q is the heat generated, was related to the reciprocal thermal conductivity of the gas in the cell by a curve determined by calibration.

The High Pressure Vessel. The high pressure vessel was constructed of SAE 4340 steel, hot rolled, and hardened to a Rockwell *C* hardness of 36.5. It was 16 inches long and had an outside diameter of 8 inches and an inside diameter of 2.5 inches. The cavity was 13 inches deep. The closure was a modified Bridgman type. A 5-inch flange was welded to the top of the bomb. This was followed by a lead gasket, a 1.5 × 10 inches reducing flange, 90° ell, and 20-inch length of 1.5-inch pipe. This arrangement allowed electrical leads to pass from the bomb to the electrical measuring equipment without coming into contact with the oil bath.

The high pressure electrodes, a critical part of the assembly, were made of ⅛-inch drill rod. Each end was threaded with a 5-40 die. On the high pressure side, hexagon nuts made from ¼-inch drill rod were screwed onto the electrodes. Electrical leads from the cell were connected to the electrodes by silver soldered lugs. Three packing washers were used, two of Supramica and one of Viton (E.I. duPont de Nemours & Co. Inc., synthetic rubber, Precision Compound No. 17009, Precision Rubber Products Corp.). The entire length of the electrodes was fitted with thin walled Teflon tubing to prevent short circuiting. Initial tightening was accomplished by means of 5-40 nuts at the outside end. The electrodes were self-tightening under pressure owing to their unsupported areas. This system is not recommended for high temperatures and pressures because many blowouts occurred during this investigation due to extrusion of the rubber gaskets. At 220° F. and 1000 atm. pressure, the gaskets failed after 6 hours. At higher temperatures, 1000 atm. could not be attained, even when the Supramica washers were machined to very close tolerances.

The oil bath (Shell Voluta No. 972 oil) was contained in a 50-gallon, jacketed copper kettle supported on a steel tripod. This oil had a flash point of 470° F., and was

[1] Present address, E.I. duPont de Nemours Co. Inc., Seaford, Del.
[2] Present address, University of Delaware, Newark, Del.

intended for use at 400° F. However, copious fumes arose from the bath at 300° F. and considerable charring occurred at the heaters. It was deemed unwise to use this oil at temperatures much higher than 300° F. An angle-iron framework was built around the kettle to support the agitator, immersion heaters, temperature controller, thermocouple probe, and bomb cradle. The high pressure vessel rested in a cradle made of two 1 × 3/16-inch flat iron straps bent into U shapes and bolted to ½-inch rods which hung freely from angle-iron supports connected to the framework.

A 1-ton Tugit chain hoist and dolly suspended from an overhead monorail allowed easy transfer of the high pressure vessel, which weighed approximately 260 pounds, into and out of the oil bath. Chromalox immersion heaters were provided to give a continuous range of heat input from 0 to 6500 watts; this proved ample for raising the bath to the desired temperature level in a reasonable time. A mercury thermoregulator (Sargent No. 58140) and relay controlled a heating arrangement which allowed a continuous range of 0 to 500 watts for on-off control. The amount of input for closest control was determined by trial and error at each temperature level. Line voltage variations to the heaters were minimized by use of constant voltage transformers. A ¼ h.p. Lightnin mixer with double propeller provided agitation of the oil bath. Temperature was controlled to within 0.04° F. about 2 inches from the bomb.

The High Pressure System. A schematic layout of the high pressure equipment is shown in Figure 2. A 20,000 p.s.i. pump (Milton-Roy), with a maximum rated capacity of 100 cc. per minute, was connected to a high-pressure U-tube arrangement. The two legs of the U-tube (Autoclave Engineers, Inc., No. 6987) were 1-liter high pressure vessels which had a working pressure of 50,000 p.s.i. at 100° F. and were connected by ¼-inch high pressure tubing. The U-tube was partially filled with triple-distilled mercury. Oil from the discharge side of the pump filled one leg of the U-tube and transmitted pressure through the mercury to the gas sample in the other leg without contaminating it. An adjustable relief valve (Aminco No. 44-9528) set at 18,500 p.s.i. and blowout assembly (Aminco) for 20,000 p.s.i. were included in the pump discharge piping circuit as shown. The intensifier was not used in these measurements.

A vacuum pump (Cenco-Hyvac) was used to purge the system, including the high pressure vessel, when fresh gas samples were introduced.

Three gages with overlapping ranges were used for measuring pressure. In the 0 to 3500 p.s.i. range, a 0 to 5000 p.s.i., 12-inch Heise-Bourdon tube gage was used; in the 3500 to 8000 p.s.i. range a 0 to 10,000 p.s.i., 8.5-inch Heise gage was used; pressures in excess of 8000 p.s.i. were measured with a Harwood Manganin pressure cell and Carey-Foster bridge which were calibrated together by the supplier to 50,000 p.s.i. The Carey-Foster bridge was powered by three dry cells (Everyready No. 6, 1.5 volt) and

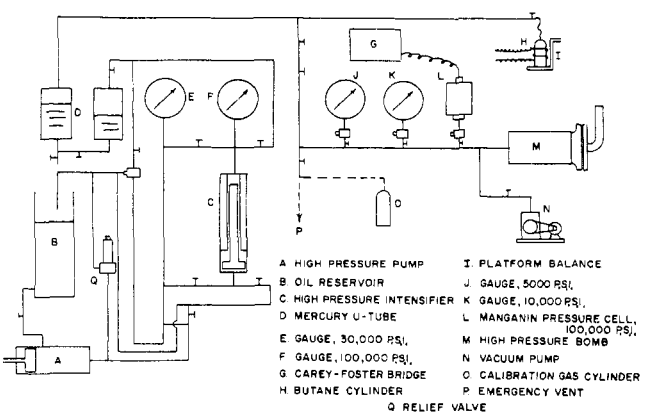

Figure 2. High pressure system

a galvanometer (Leeds and Northrup No. 2430) was used in conjuction with it. The Heise gages were calibrated with a dead weight gage. The low range gage was marked in 10 p.s.i. divisions, so that readability was ±1 p.s.i. The intermediate range gage was marked in 20 p.s.i. divisions, so that readability was to the nearest 5 p.s.i. The pressure dial on the Carey Foster bridge was marked in 100 p.s.i. divisions with readability to the nearest 20 p.s.i. Each gage was protected by a suitable blowout assembly. Calibration of the gages indicated that gage readings were accurate to 0.5% without further correction.

Electrical Equipment. The platinum coil was wired in series with a 10-ohm standard resistor (Leeds and Northrup No. 4025-B). This resistor was kept in an enclosed, insulated oil bath. Thermocouple electromotive force (e.m.f.) and potential difference readings across the standard resistor and the platinum coil were taken with a potentiometer (Leeds and Northrup K-2). Potential differences of more than 1.6 volts were measured by tapping off 0.1 of the voltage from a volt box (Rubicon Ser. No. 56545). Standard current was supplied to the potentiometer by a 6-volt storage cell wired in series with a 150-ohm carbon-filled resistor. A galvanometer (Leeds and Northrup No. 2500) sensitivity 0.39 μa. per mm. and a standard cell were used. Sensitivity and readability were such that in most instances voltages to ±1 in the fifth figure could be reproduced.

The Calibration Curve. The flow of heat from the platinum coil to the oil bath can be described by the equation

$$Q = \frac{-\Delta t}{R} \tag{1}$$

where R is the sum of all the thermal resistances. These resistances may be analyzed in a manner analogous to electrical resistances. When this is done, the equivalent resistance R is found to be a function of the geometry and thermal conductivities of the copper cylinders, Supramica insulators, and gas sample. The cell is designed to minimize all thermal resistances relative to the resistance of the gas sample, so that Equation 1 takes the form

$$-\frac{\Delta t}{Q} \approx \frac{f(t)}{k} \tag{2}$$

where $f(t)$ represents the geometrical factor, which is temperature dependent. A plot of $-\Delta t/Q$ *vs.* $1/k$ should be nearly linear at constant temperature.

By measuring $-\Delta t/Q$ for several different gases of known k, the exact relationship between $-\Delta t/Q$ and $1/k$ can be determined. Because of the approximate linearity of the relationship, relatively few gases are required for calibration. A curve of this type is required at each temperature level.

Use of the calibration curve at elevated pressures requires that the geometry of the cell and the thermal conductivities of the construction materials remain essentially constant, while the only change with pressure is the thermal conductivity of the gas sample. Thermal conductivities of solids change only slightly with pressure, and since these thermal resistances are as high or as low as required, second order changes in their conductivities do not affect the calibration curve. The most important part of the geometry of the cell is the gas layer thickness. An analysis of the radial displacements of the copper cylinders under a hydrostatic pressure of 20,000 p.s.i. indicates that an error of about 0.1% is incurred by neglecting this effect.

EXPERIMENTAL

Experimental Procedure. After evacuating the bomb one of the calibration gases was introduced at approximately 300 p.s.i. and then bled off to 1 atm. This rinsing cycle was repeated four times and the final rinse was bled off to 1 atm. The system was allowed to come to thermal equilibrium. A nominal current of 3 ma. was then passed through

platinum wire, across the standard 10-ohm resistance in series with it, and of the thermocouple. When the readings were constant, thermal equilibrium had been established. Another 20 minutes at least were allowed before resistance measurements were made. After equilibrium measurements had been recorded, a current of 0.1 to 0.25 amp. was caused to flow through the platinum heater. When a steady-state heat transfer from wire to bath was attained, platinum resistance and thermocouple potential values were again recorded. These were repeated five times at intervals of a few minutes. Experience indicated that approximately 1 hour each was required for attainment of equilibrium and of steady-states; readings were commenced after this period.

This procedure was repeated with three other calibration gases which covered the range of thermal conductivities of interest, and a plot of $1/k$ *vs.* $\Delta t/Q$ was made. The gas under investigation was then introduced into the system, using the same steps as for flushing. In the case of butane, whose vapor pressure at room temperature is only 19 p.s.i., the flushing procedure was repeated eight or nine times. The pressure of the gas was raised to the desired level, and equilibrium and steady-state measurements were made. From these measurements, $\Delta t/Q$ was calculated, and $1/k$ was determined from the calibration curve.

The gases used for calibration were: helium (Matheson Co., instrument grade, 99.99% minimum); methane (Matheson Co., C.P. grade, 99.0% minimum); nitrogen (Matheson Co., instrument grade, 99.996% minimum); carbon dioxide (Liquid Carbonic Corp., Saf-Dry, 99.99%). Butane (Matheson Co., instrument grade, 99.5% minimum) was used. The stated percentages of purity are manufacturer's specification, and were accepted without analyses. Nitrogen measurements were made with the same gas as for calibration.

Calculation of $\Delta t/Q$. The international formula relating the electrical resistance of platium wire to temperature is:

$$R = a + bt + ct^2 \tag{3}$$

where R = resistance and $a, b, c,$ = constants. Let ΔR be the difference in resistances between steady state and equilibrium readings.

$$\Delta R = R_2 - R_1 = b(t_2 - t_1) + c(t_r^2 - t_1^2)$$
$$= b(t_2 - t_1) + c(t_2 - t_1)\,(t_2 + t_1)$$
$$= b\,\Delta t + 2c(\Delta t)\,t_{\text{av.}}$$

and

$$[(\Delta t)_{s\,-\,e}]_{pt} = \frac{\Delta R}{b + 2ct_{\text{av.}}} \tag{4}$$

The quantity $[(\Delta t)_{s\,-\,e}]_{pt}$ represents the difference between steady-state and equilibrium values of temperature. The constants b and c determined by calibration at fixed temperature points were:

$$b = 0.01404_2 \qquad c = -9.1_1 \times 10^{-9}$$

with t in ° F. and $t_{av.}$ expressed as ° F. above 32°.

The thermocouple was calibrated at the same temperature points, and the e.m.f. were quite close to tabulated values. The temperature difference was therefore taken as the difference between e.m.f. at steady-state and equilibrium divided by the slope of the temperature-e.m.f. curve as indicated by the thermocouple tables at the particular temperature level. In the steady state case, the temperature difference between the platinum heater and the thermocouple was

$$\Delta t = [\Delta t_{s\,-\,e}]_{pt} - [\Delta t)_{s\,-\,e}]_{tc} \tag{5}$$

This procedure eliminated effects of resistance and e.m.f. changes of the platinum wire and thermocouple with pressure. It was assumed that dR/dt and $d(\text{e.m.f.})/dt$ were not affected by pressure. The calculation of $[\Delta t_{s\,-\,e}]_{pt}$ was insensitive to oil bath temperature. Resistances were measured to five figures, with an uncertainty of ± 1 in the fifth figure. The factor ΔR was thus known to three figures with an uncertainty of ± 2 in the third figure. The magnitude of ΔR was about 4, so that an uncertainty of about 0.5%, or ± 0.02° F. prevailed in the calculation of $[\Delta t_{s\,-\,e}]_{pt}$. The quantity $[\Delta t_{s\,-\,e}]_{tc}$ which was about 0.3° F. was calculated to two figures, with an uncertainty of ± 0.01° F. Therefore, Δt had an uncertainty of ± 0.03° F. or about 1%. The heat input Q was calculated as E^2/R where E was the potential across the platinum wire. Since both E and R were measured to five figures, Q was known to at least four significant figures. Thus, Δt was the limiting factor and $\Delta t/Q$ had an uncertainty of 1%. The calibration curves showed that errors of this order of magnitude in $\Delta t/Q$ caused errors in $1/k$ of from 1 to 2%. It is estimated that the approach to steady-state conditions also set similar limits.

Convection can usually be noted, when it is present, by anomalous behavior such as the peak in the 327° F. isotherm shown in Figure 3. Spot measurements with as much as a fourfold change in Δt did not reveal the presence of convection.

Range of Conditions and Results. The thermal conductivity of nitrogen was measured at 167.5° F. (75° C.) and up to 1000 atm. so that results could be compared with those of others. Results of the nitrogen data (Table I) agree within 2 to 3% with the more acceptable data in the literature (*5, 6*).

The thermal conductivity of butane was measured at 167° F. and 22° F. from 1 to 1000 atm., at 285.5° F. from 1 to 850 atm., and at 327° F. from 1 to 500 atm. The results are shown in Table II and in Figures 3 and 4.

DISCUSSION OF RESULTS

The measurements on butane are plotted in Figures 3 and 4 as thermal conductivity *vs.* pressure, at constant temperature. The isotherms in these figures represent smoothed

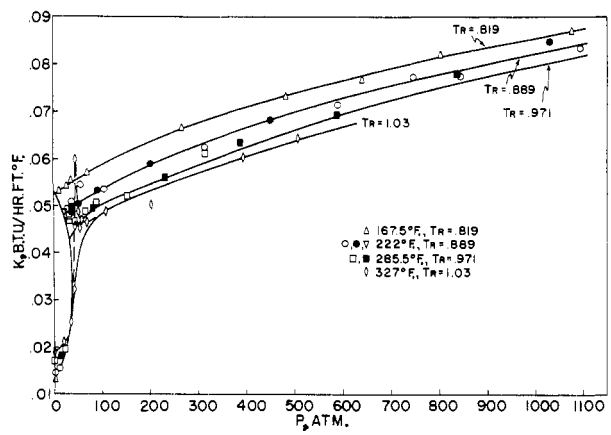

Figure 3. Thermal conductivity of butane *vs.* pressure

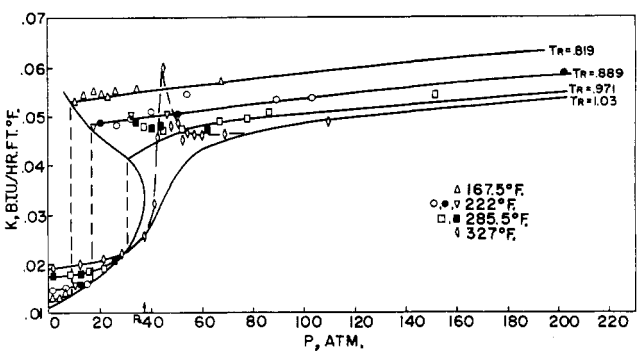

Figure 4. Thermal conductivity of butane *vs.* pressure

Table I. Nitrogen Thermal Conductivity

Temp., ° F.	Pressure, Atm.-Abs.	k, B.t.u. / Hr. × Ft. × ° F.
167.5	105.1	0.0200
	201.9	0.0229
	387.8	0.0291
167.5	200.4	0.0229
	390.1	0.0283
	613.2	0.0364
	792.8	0.0408
	1021.4	0.0481

data taken from a plot of residual thermal conductivity $k - k^*$ *vs.* density (Figure 5). Irregularities in the data were smoothed in the residual conductivity-density charts.

A smooth curve was drawn through the gas and liquid data of Figure 5. The portion of the curve through the gas data (at densities less than 10 pounds per cubic foot) was drawn as a straight line passing through the coordinates $[\log (k - k^*)]_{av.}$ and $(\log \rho)_{av.}$ for the gas data alone. It is seen in the work of Vargaftik (*24*) that straight lines result in this region for similar plots of water, carbon dioxide, oxygen, nitrogen, hydrogen, and methane. Large deviations from the smooth curve of Figure 5 are observed near the critical density, corresponding to the peak in the 327° F. isotherm and the rise in the 285.5° F. isotherm shown in Figures 3 and 4. The data taken at 327° F. near the critical pressure can be explained in terms of convection.

If a least squares method had been employed in Figure 5 for determining the slope of the straight line portion of the curve, a straight line would have resulted which would have passed through the coordinates $[\log (k - k^*)]_{av.}$, $(\log \rho)_{av.}$ for ρ less than 10 pounds per cubic foot. It would have a slope that would not necessarily make it connect with the lower end of the curve through the high density data. Because experience indicates that a single continuous curve should pass through both low and high density data, the straight line portion of the curve was drawn so that it passed through the low density average ordinates and connected to the lower end of the high density curve. This line was taken to be the best fit of the low density data. The same procedure was used in determining the slope of the straight line portion of the residual conductivity-density curve for propane in Figure 6.

It is seen, Figures 3 and 4 that the thermal conductivity of gasous butane below the critical pressure increases with pressure and temperature. In the liquid phase, the thermal conductivity increases with pressure, but decreases with temperature. Small humps appear in the 167.5° and 222° F. isotherms in the liquid phase near the bubble point. The 285.5° F. isotherm shown in Figure 4 exhibits a single large rise near the two-phase region. Similar humps are observed in the propane data of Leng (*10, 11*) at $T_R = 0.875$, 0.921, and 0.974; they exhibit maxima near the critical pressure and decrease in size as the temperature increases up to the critical. In comparison, butane exhibits double humps at $T_R = 0.819$ and 0.889 and a single rise at $T_R = 0.971$. The humps are smaller in magnitude, have maxima at different pressures, and get larger as the critical temperature is approached. The humps may be due to instability of the liquid phase in the region of the bubble point.

Moore, Gibbs, and Eyring (*18*) demonstrated that liquids undergo transitions other than solid-liquid and liquid-gas transitions. Evidence points to a substantial degree of order in liquids and indicates that changes in molecular array correspond to changes in physical properties. The dimensions of the butane molecule are given as 4.0 × 4.9 × 7.78 A., so that for a cubic nonrotating arrangement of molecules, the molecular volume is calculated to be 152 A.^{3}, corres-

Table II. Butane Thermal Conductivity

Temp., ° F.	Pressure, Atm.-Abs.	k, B.t.u. / Hr. × Ft. × ° F.
167.5	1	0.0130
	3.7	0.0131
	6.1	0.0140
	8.48	0.0813
	8.48	0.0741
	10.39	0.0529
	13.9	0.0546
	17.7	0.0550
	20.9	0.0546
	23.2	0.0540
	26.2	0.0552
	35.0	0.0556
	68.1	0.0571
	267.3	0.0666
	482.0	0.0730
	640.5	0.0764
	803.7	0.0819
	1077.0	0.0870
	1	0.0148
	6.3	0.0150
	14.2	0.0158
	21.3	0.0490
	26.7	0.0483
	32.2	0.0495
	40.5	0.0510
	54.2	0.0546
	103.2	0.0536
	315.3	0.0625
	591.1	0.0715
	845.2	0.0775
	1095.0	0.0833
222	1	0.0145
	9.84	0.0156
	18.0	0.0479
	32.2	0.0504
	47.1	0.0508
222	1	0.0146
	12.4	0.0157
	20.5	0.0488
	50.6	0.0505
	89.6	0.0533
	202.0	0.0590
	451.3	0.0680
	747.9	0.0772
	1029.0	0.8047
285.5	1	0.0174
	8.14	0.0178
	15.4	0.0187
	21.7	0.0195
	28.0	0.0217
	34.0	0.0495
	35.0	0.0481
	36.9	0.0470
	37.2	0.0482
	38.6	0.0476
	42.4	0.0474
	44.9	0.0472
	52.1	0.0476
	67.2	0.0491
	86.7	0.0509
	151.7	0.0545
	314.6	0.0614
285.5	1	0.0174
	12.5	0.0179
	25.4	0.0209
	32.2	0.0500
	34.5	0.0490
	36.7	0.0479
	38.4	0.0473
	40.8	0.0477
	44.1	0.0483
	62.4	0.0473
	78.1	0.0495
	232.6	0.0563
	391.1	0.0635
	590.8	0.0692
	838.4	0.0781
327	1	0.0191
	12.0	0.0200
	21.3	0.0211
	28.8	0.0220
	37.3	0.0255
	41.6	0.0322
	43.1	0.0459
	45.5	0.0599
	48.3	0.0481
	50.0	0.0493
	50.7	0.0488
	52.8	0.0455
	54.8	0.0470
	57.1	0.0463
	60.5	0.0467
	69.2	0.0465
	109.8	0.0488
	205.7	0.0503
	397.3	0.0602
	509.8	0.0645

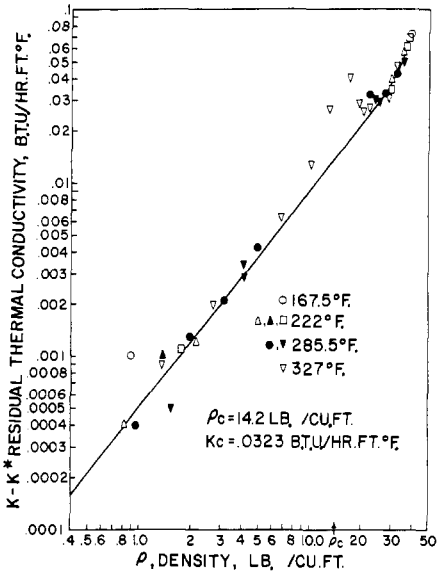

Figure 5. Residual thermal conductivity of butane *vs.* density

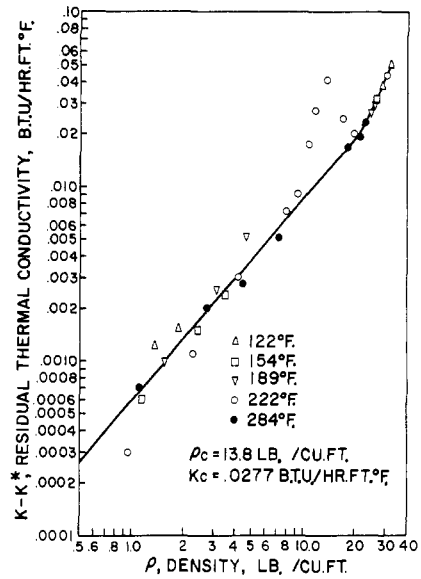

Figure 6. Residual thermal conductivity of propane *vs.* density

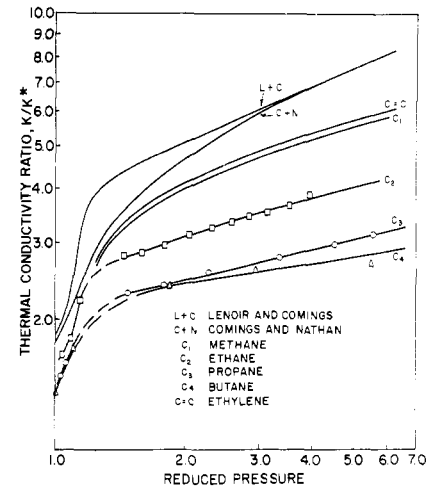

Figure 7. Comparison of methane, ethane, propane, and butane with correlations at T_R = 1.03

ponding to a density of 39.7 pounds per cubic foot. For a cubic arrangement in which the molecules rotate about their long axes, the molecular volume is 187 A.^{3}, corresponding to a density of 32.3 pounds per cubic foot. For a hexagonal rotating arrangement the molecular volume is 162 A.^{3}, corresponding to 37.3 pounds per cubic foot. It is seen in Figure 5 that a sudden change of slope occurs in the residual conductivity-density curve at a density of about 32 pounds per cubic foot and that it is in this region that humps occur in the various isotherms. A possible explanation is that in this region the molecules are trying to attain some order, but are unable to until displaced further from the bubble point by application of more pressure. They then assume a cubic arrangement with full rotation about their long axes. A transition from cubic to hexagonal packing should occur at a density of 37.3 pounds per cubic foot. It is expected that a nonrotating cubic arrangement prevails at still higher densities.

The three liquid-phase isotherms are approximately parallel and linear when plotted as log k *vs.* log density. At densities greater than 32 pounds per cubic foot the common slope is 2.2. This slope may be compared with that predicted by Bridgman's equation for thermal conductivities of liquids at high pressures (*1*). His equation is:

$$k = \frac{3R}{N}\,\bar{a}\,D^{2} \qquad (6)$$

Substituting Rao's (*21*) empirical expression for the velocity of sound $\bar{a}$, and $(m/\rho)^{1/3}$ for D gives

$$k = \left(\frac{3R}{N}\right)\left(\frac{\rho^3 R'^3}{M^3}\right)\left(\frac{\rho}{m}\right)^{2/3}$$

$$= \frac{3RR'^3}{N^{1/3}M^{11/3}}\,\rho^{11/3}$$

$$= \text{constant}\,\rho^{3.7} \qquad (7)$$

It can be concluded from Equation 7 that if Rao's expression is valid, then Equation 6 has too heavy a dependence on density. Predicted values for alcohols at 12,000 kg. per cc. are as much as 50% higher than experimental values (*1*).

The 327° F. isotherm (Figures 3 and 4) shows a peak at a pressure slightly greater than the critical. This behavior was also observed by Leng at T_R = 1.03 for propane. Using the product of the Grashof and Prandtl numbers as a criterion of convection, Leng found that convection was imminent for propane under these conditions with the Δt used in his experiments. A similar plot $(Gr)(Pr)/\Delta t$ *vs.* pressure for butane at 327° F. showed that in a region slightly past the critical pressure, Δt of 3° F. gave a value of $(Gr)(Pr)$ of about 600 and convection was predicted.

The value of the thermal conductivity of butane at the critical point was estimated from Figure 5. The value of $(k_c - k_c^*)$ was taken from the curve at the critical density, and k_c^* was determined by extrapolation of the 1 atm. measurements. The thermal conductivity at the critical point is 0.0323 B.t.u. per hour per foot per ° F.

CORRELATION OF RESULTS

Correlation of High Pressure Butane and Propane Data. Figure 5 may be used to predict thermal conductivity values for butane at any combination of temperature and pressure for which the density is between 0.3 and 40 pounds per cubic foot. Densities may be obtained (*22*) and k^* can be determined at any temperature by linear extrapolation on a plot of log k^* *vs.* log temperature. Values obtained from Figure 5 are expected to have an accuracy of 2%. The similar plot for propane constructed from Leng's (*10, 11*) data and shown in Figure 6 allows extrapolation of the propane data within the density limits 1.0 to 32 pounds per cubic foot. Densities may be obtained from (*23*) and k^* can hour per foot per ° F. for propane. Density values used to construct the propane chart were from other data (*15*).

Generalized Correlation at High Pressure. It was pointed out by Leng that ethane and propane show large deviations from each other and from the Comings and Nathan correlation when plotted as thermal conductivity ratio k/k^* *vs.* reduced pressure at reduced temperatures of 1.03 and 1.11. Figure 7 is such a plot at T_R = 1.03, comparing the Comings and Nathan (*4*), and Lenoir and Comings (*13*) correlations with methane (*19*), ethane (*14*, Table V), propane (*12*), butane, and ethylene. Curves for methane and ethylene were taken for generalized charts for these substances (*19, 20, 23*). The butane and propane curves in Figure 7 lie close together, but diverge at higher pressures; at P_R = 5.0, k/k^* for butane is 8% lower than k/k^* for propane. It is evident that two parameters are insufficient to correlate thermal conductivity ratios for complex molecules.

Considering the dense gas to have a liquid-like structure,

an extension of the Kincaid and Eyring (8) expression indicates that the thermal conductivity ratio, k/k^*, is a function of the three variables, T_R, P_R, and C_p^* for those substances whose volumetric behavior is similar. The use of C_p^* as a third variable should be an improvement over the f factor suggested by Leng, because heat capacity reflects the degrees of vibrational freedom which are active at the temperature level of interest, whereas f does not. The factors f and C_p^* should be equivalent as correlating parameters at high temperatures. A plot of k/k^* values for various hydrocarbon gases at $T_R = 1.03$ *vs.* C_p^* is shown in Figure 8.

CONCLUSIONS

A thermal conductivity cell was developed and operated successfully up to pressures of 1000 atm. and at temperatures up to 327° F. Butane measurements were made at reduced temperatures of 0.819, 0.899, 0.971, and 1.03, and at

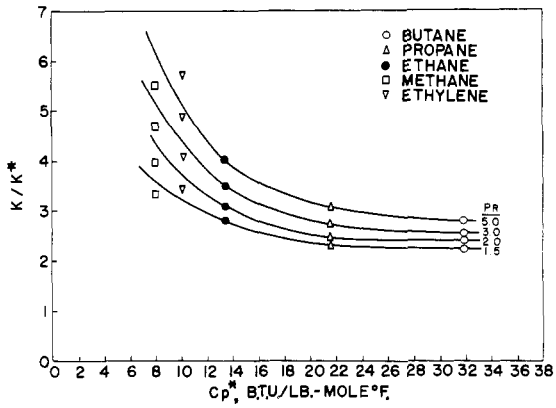

Figure 8. Thermal conductivity ratio *vs.* heat capacity at $T_R = 1.03$

pressures up to 28 times the critical pressure. The measurements are believed to have an accuracy of 2%. The thermal conductivity of nitrogen was measured at 75° C. and up to 1000 atm. and was found to agree within 2 to 3% with the more acceptable data in the literature.

Near the bubble point, the thermal conductivity of liquid butane exhibits small humps which are interpreted as an instability of the liquid phase close to the two phase region. It is demonstrated that a two parameter, generalized correlation for thermal conductivity ratio is insufficient for more complex molecules near the critical region. On the basis of the available data, it is demonstrated that C_p^*, the heat capacity at 1 atm., is suitable as a third parameter in generalized correlations of thermal conductivity ratio for the hydrocarbons.

NOMENCLATURE

- $\bar{a}$ = velocity of sound
- C_p^* = heat capacity at constant pressure at 1 atm.
- D = intermolecular distance in cubic array
- f = vibrational degrees of freedom
- k = thermal conductivity
- k_c = thermal conductivity at the critical point
- k^* = thermal conductivity at 1 atm.
- k_c^* = thermal conductivity at 1 atm. and the critical temperature
- M = molecular weight
- m = mass of a molecule
- N = Avogadro's number
- p = pressure
- p_c = critical pressure
- P_R = reduced pressure, p/p_c
- Q = heat transferred per unit time
- R = gas constant, also resistance
- R_1 = resistance at equilibrium
- R_2 = resistance at steady-state
- R' = Rao's constant
- T_R = reduced temperature = t/t_c
- t = temperature, t_c = critical temperature
- ρ = density
- ρ_c = critical density
- Δ = difference

ACKNOWLEDGMENT

The financial assistance provided by the national Science Foundation, the Visking Corp., E.I. du Pont de Nemours & Co., Inc., and Esso Research and Engineering Co. is gratefully acknowledged.

LITERATURE CITED

(1) Bridgman, P.W., "The Physics of High Pressure," Bell and Sons, Ltd., London (1952).
(2) Chapman, S., Cowling, T.G., "The Mathematical Theory of Non-Uniform Gases," Cambridge Univ. Press, Cambridge, Eng., 1939.
(3) Comings, E.W., Lee, W., Kramer, F.R., Proc. Joint Conf. on Thermodynamics and Transport Properties, London, July 1957, p. 188, Inst. Mech. Engrs., London, 1957.
(4) Comings, E.W., Nathan, M.F., *Ind. Eng. Chem.* **39**, 964 (1947).
(5) Johannin, P., Proc. Joint Conf. on Thermodynamic and Transport Properties of Fluids, London, July 1957, p. 193, Inst. Mech. Engrs., London, 1957.
(6) Johannin, P., Vodar, B., *Ind. Eng. Chem.* **49**, 2040, (1957).
(7) Junk, W.A., Jr., PhD. thesis, University of Illinois, Urbana, Ill., 1952.
(8) Kincaid, J.F., Eyring, H., *J. Chem. Phys.* **6**, 620 (1938).
(9) Lee, W., M.S. thesis, Purdue University, Lafayette, Ind., 1956.
(10) Leng, D.E., PhD. thesis, Purdue University, Lafayette, Ind., 1956.
(11) Leng, D.E., Comings, E.W., *Ind. Eng. Chem.* **49**, 2042 (1957).
(12) Lenoir, J.M., Ph.D. thesis, University of Illinois, Urbana, Ill., 1949.
(13) Lenoir, J.M., Comings, E.W., *Chem. Eng. Progr.* **47**, 223 (1951).
(14) Lenoir, J.M., Junk, W.A., Comings, E.W., *Ibid.*, **49**, 539 (1953).
(15) Lydersen, A.L., Greenkorn, R.A., Hougen, O.A., "Generalized Thermodynamic Properties of Pure Fluids," University of Wisconsin Eng. Expt. Sta. Rept. 4, (1955).
(16) Michels, A., Botzen, A., *Physica* **18**, 605 (1952); **19**, 585 (1953).
(17) Michels, A., Cox, J.A.M., Botzen, A., Friedman, A.S., *J. Appl. Phys.* **26**, 843 (1955).
(18) Moore, R.J., Gibbs, P., Eyring, H., *J. Phys. Chem.* **57**, 172 (1953).
(19) Owens, E.J., Thodos, G., Proc. Joint Conf. on Thermodynamics and Transport Properties of Fluids, London, July 1957, p. 163, Inst. Mech. Engrs., London, 1957.
(20) Owens, E.J., Thodos, G., Natl. Meeting A.I.Ch. E., Preprint 25, St. Paul, Minn., September 27-30, 1959.
(21) Rao, R.J., *J. Chem. Phys.* **9**, 682 (1941).
(22) Sage, B.H., Lacey, W.N., "Thermodynamic Properties of the Lighter Paraffin Hydrocarbons and Nitrogen," Am. Petrol. Inst., New York, 1950.
(23) Schaefer, Charles A., Thodos, G., *A.I.Ch.E. Journal* **5**, 367 (1959).
(24) Vargaftik, N., Proc. Joint. Conf. Thermodynamic and Transport Properties of Fluids, London, July 1957, p. 148, Inst. Mech. Engrs., London, 1957.

RECEIVED for review November 11, 1959. Accepted June 30, 1960. Based in part on a thesis presented by E.R. Kramer in partial fulfillment of the requirements for the Ph.D. degree in chemical engineering, Purdue University, Lafayette, Ind., 1959. Microfilm copy available from University Microfilm Inc., Ann Arbor, Mich. Division of Industrial and Engineering Chemistry, 136th Meeting, ACS, Atlantic City, N.J., September 1959.